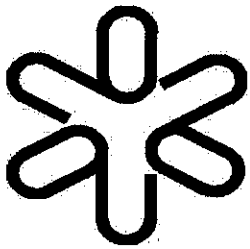

Instituto de Física
Universidade de São Paulo

Ray-tracing of the Schmidt Camera with Corrector Plate

Sato, R. and Bellido C., J.A.
Departamento de Física Nuclear, Instituto de Física, Universidade de São Paulo, São Paulo, Brasil

Reis, H.C.
Departamento de Raios Cósmicos e Cronologia, Universidade Estadual de Campinas, São Paulo, Brasil

Publicação IF - 1400/2000

Ray-tracing of the Schmidt Camera with Corrector Plate

R. Sato* *and* J. A. Bellido C.†

Departamento de Física Nuclear

Universidade de São Paulo - USP

CP 66318, 05315-970 São Paulo - SP, Brazil

H. C. Reis‡

Departamento de Raios Cósmicos e Cronologia

Universidade Estadual de Campinas - Unicamp

CP 6165, 13083-970, Campinas - SP, Brazil

GAP-99-012

Abstract

In this work we developed a ray-tracing program to simulate the optic of the Schmidt camera of the Auger project fluorescence detector. We placed corrector plates on the camera in order to decrease the size of the spot of light reflected at the phototubes surface, coming from extensive air showers. In addition, we discuss the presence of shadows projected by the cluster within the diagrams of the spot.

1 Introduction

One of the tasks of the Auger Project Fluorescence's [1] group is to determine if the Schmidt camera should be installed with a corrector plate at the diaphragm aperture. It is already known that this optical element decrease notoriously the spheric aberration [2]. In a recent work [3], Matthiae and Privitera showed that using a corrector plate we get a sensible decreasing of the spot size, improving the optical quality of the Schmidt system.

In this work we want to show the ray-tracing program that was performed in order to simulate all the optic of the Schmidt camera (this means with or without corrector plate)

*rsato@charme.if.usp.br

†jabca@charme.if.usp.br

‡hreis@ifi.unicamp.br, hreis@charme.if.usp.br

and study the behavior of the spot size as a function of the incidence angle. In addition, we can study the shadow on the mirror projected by the cluster of phototubes. In the case of a Schmidt camera with corrector plate, we can chose between two kind of lens [2].

This work is divided in the following way: Section II has a brief description of our program and of the parameters used to simulate the camera. Section III and IV have the simulation results (with and without corrector plate) and the analysis of this results, respectively. In section V we discuss the presence of shadows projected by cluster on the mirror. In section VI we draw our conclusions.

2 Description of the Program

The Optical system simulated here is showed in figure 1 ($R = 3.4m$ and $Dd = 1.7m$). We considered a spherical cluster with 20×20 hexagonal phototubes. The size of the cluster is designed in order to cover $30^o \times 30^o$ field of view in the sky ($1.5^o \times 1.5^o$ per pixel). This means that the size of the cluster should change if we change the value of any parameter of the Schmidt camera, in order to keep the aperture view of $30^o \times 30^o$

2.1 Algorithm of the Program

Following we describe each step of the program:

- Given the incidence direction of the light ($\hat{i}$), the program chose randomly the vector position ($\vec{r_o}$) above the diaphragm aperture.
- When we consider the corrector plate, we have to calculate the new direction of the incident vector after crossing the corrector plate ($\vec{n_l}$), and the point where the ray leaves the second surface ($\vec{r_l}$) of the lens. In each surface of the corrector plate we used the Snell law.
- With the direction $\hat{i}$ ($\vec{n_l}$ when using corrector plate) and the position $\vec{r_o}$ ($\vec{r_l}$ when using corrector plate) the program find the intersection of this ray with the focal surface. If this point were above the region defined by the phototubes, the program returns to step one until the ray were not blocked by the cluster of phototubes.
- Next step is to calculate the intersection point of the ray inside the camera and the mirror surface. This point is given by a vector position ($\vec{r_e}$) witch origin is placed on the mirror vertices. Using the reflection law, we calculate the direction of the ray reflected by the mirror ($\vec{n_e}$).
- The last point to be calculated is the intersection point of the ray reflected by the mirror at the position $\vec{r_e}$ and direction $\vec{n_e}$ with the focal surface.

This process is repeated until we have the desired number of rays. It is important to mention that there were not simulated possibles partial reflections at the corrector plate surfaces neither absorption effects at the corrector plate or at the mirror.

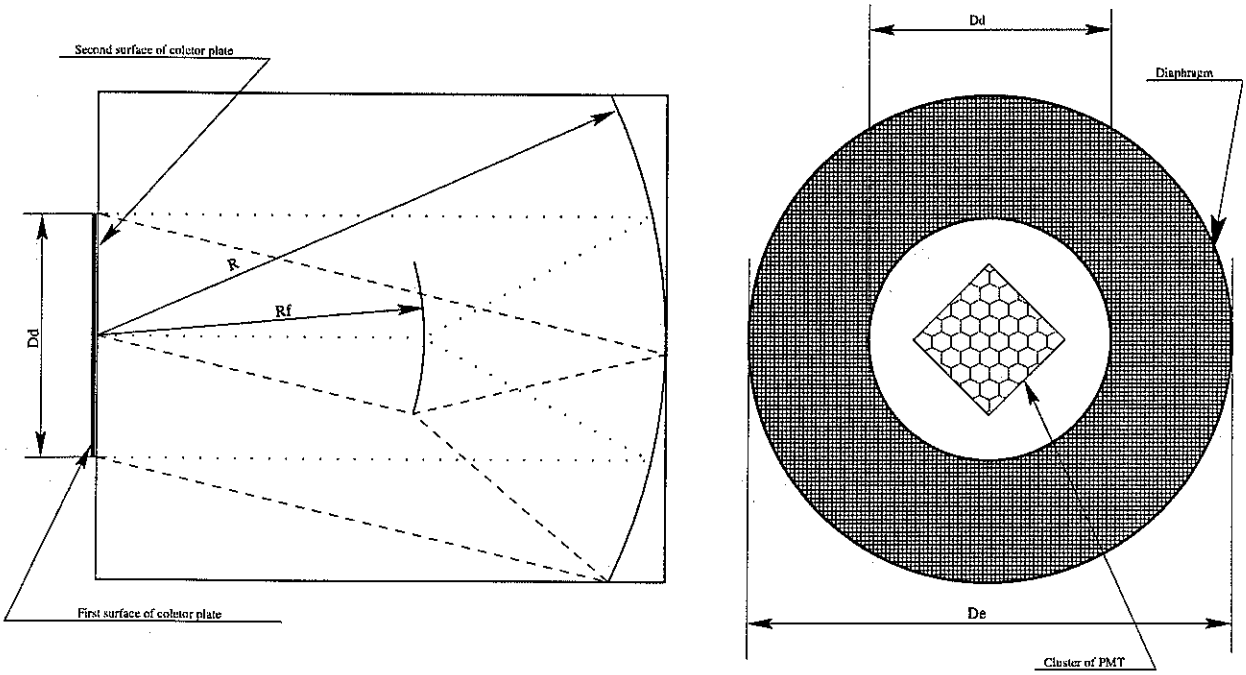

Figure 1: Schmidt camera's geometry

As we said before, when we simulate the diaphragm with a corrector plate we can choose between two lens, these two kind of lens are the same to the lens in ref. [2]:

Corrector plate type I:

$$T(r) - T(0) = \frac{r^4}{32(n-1)f^3} \ , \tag{1}$$

where $T(r)$ is the thickness of the lens as a of the distance r to its axis, n is the refraction index of the material[1]. The thickness of the lens at the core is given by $T(0)$ (for a lens given by equation 1, $T(0) = 5\text{mm}$), f is the focal distance ($f = 1.706m$).

Corrector plate type II:

$$T(r) - T(0) = \frac{r^4 - Ar^2}{32(n-1)f^3} \ . \tag{2}$$

Here A is a fixed value

$$A = \frac{3}{2} {R_{dia}}^2 \ , \tag{3}$$

where R_{dia} is the diaphragm's radius. The objective is to minimize the chromatic aberration [2] (for this lens, the value of $T(0)$ and f are $10mm$ and $1.743m$, respectively.

[1] In this case, we used glass, $n = 1.5$

3 Details of the Simulation

In Our simulation, the curvature radius of the focal surface (R_f) was estimated in order to have the minimum spot size for an incidence angle of zero degrees, without considering the region obscured by the PMT's. Furthermore, the radius of the spot size was defined as the radius that enclose 90% of the photons arriving to the focal surface.

The geometry for the Schmidt camera that we simulated is showed in figure 1, considering incidence angles of 0^o (dotted line) and 20^o (dashed line). The projection of the spot size at the focal plane and its radial distribution considering the Schmidt camera without and with corrector plate type I and II, are showed in figures 2-4, respectively. In table 1 we have the spot size (radius of the spot) as a function of the incidence angle.

Another important quantity analyzed in this work is the effective area of the optical system of the fluorescence detector. Suppose that θ is the incidence angle. In this way, $N_o cos\theta$ is the number of rays that cross the diaphragm aperture, where N_o is the number of rays that cross the diaphragm aperture with $\theta = 0^o$. The observed effective area, A_{eff}, is approximately proportional to the number of rays, n, that reached the focal surface without being blocked by the cluster of PMT's:

$$\frac{A_{eff}}{A_d cos\theta} = \frac{n}{N_o cos\theta} \quad \longrightarrow \quad A_{eff} = A_d \frac{n}{N_o} \ , \tag{4}$$

where A_d is the aperture area of the diaphragm. It is considered that the decreasing of this area is a function of the incidence angle and of the obscured area by the PMT's.

	Without corrector plate		With corrector plate I		With corrector plate II	
	$R_{foc} = 1.743m$		$R_{foc} = 1.706m$		$R_{foc} = 1.743m$	
angle	Radius	Radius	Radius	Radius	Radius	Radius
$(degree)$	(mm)	$(degree)$	(mm)	$(degree)$	(mm)	$(degree)$
0.	6.92	0.23	1.51	0.051	1.21	0.040
5.	7.38	0.24	1.59	0.053	1.19	0.040
10.	7.46	0.25	1.99	0.067	1.19	0.040
15.	7.48	0.25	3.24	0.109	1.51	0.050
20.	7.50	0.25	4.92	0.165	2.08	0.068

Table 1: Spot size as a function of several angles of incidence

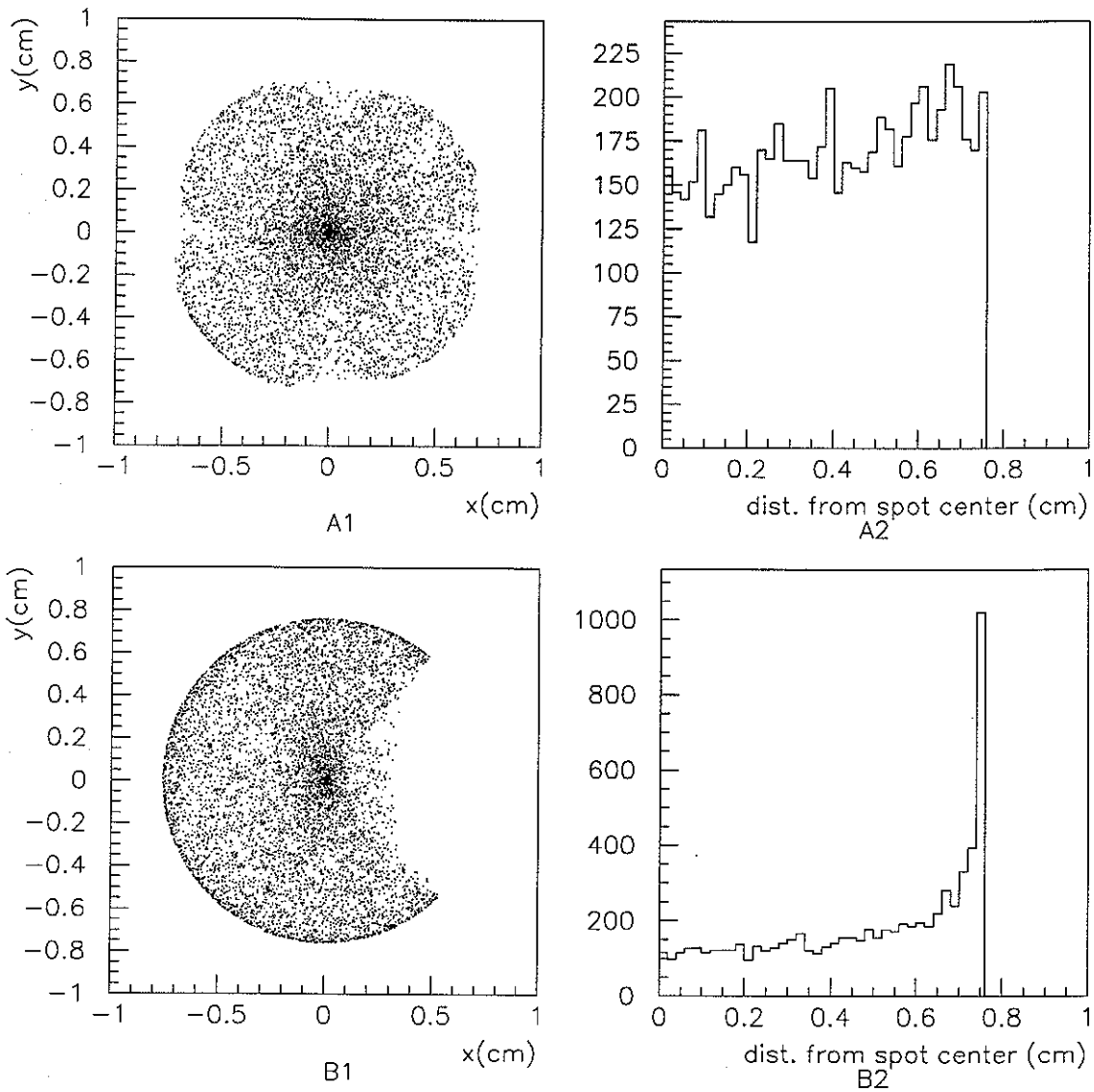

Figure 2: Projection of figure of the spot on the spherical PMT's cluster at the focal plane for a Schmidt camera without corrector plate, with incidence angles of 0^o (fig .A1) and 20^o (fig .B1). Figures A2 and B2 are the corresponding radial distribution of the spot size.

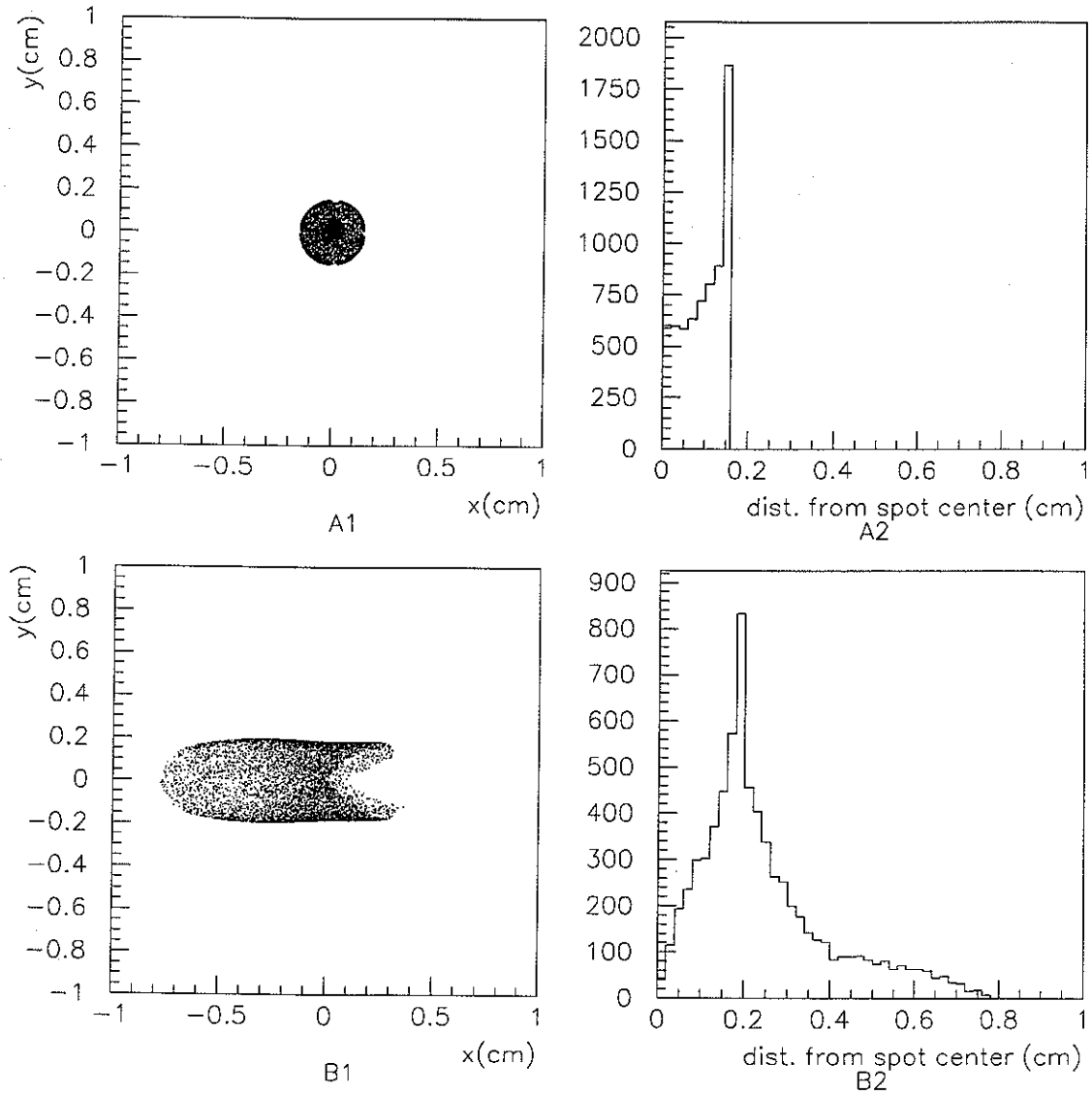

Figure 3: Projection of figure of the spot on the spherical PMT's cluster at the focal plane for a Schmidt camera with corrector plate type I, with incidence angles of 0^o (fig .A1) and 20^o (fig. B1). Figures A2 and B2 are the corresponding radial distribution of the spot size.

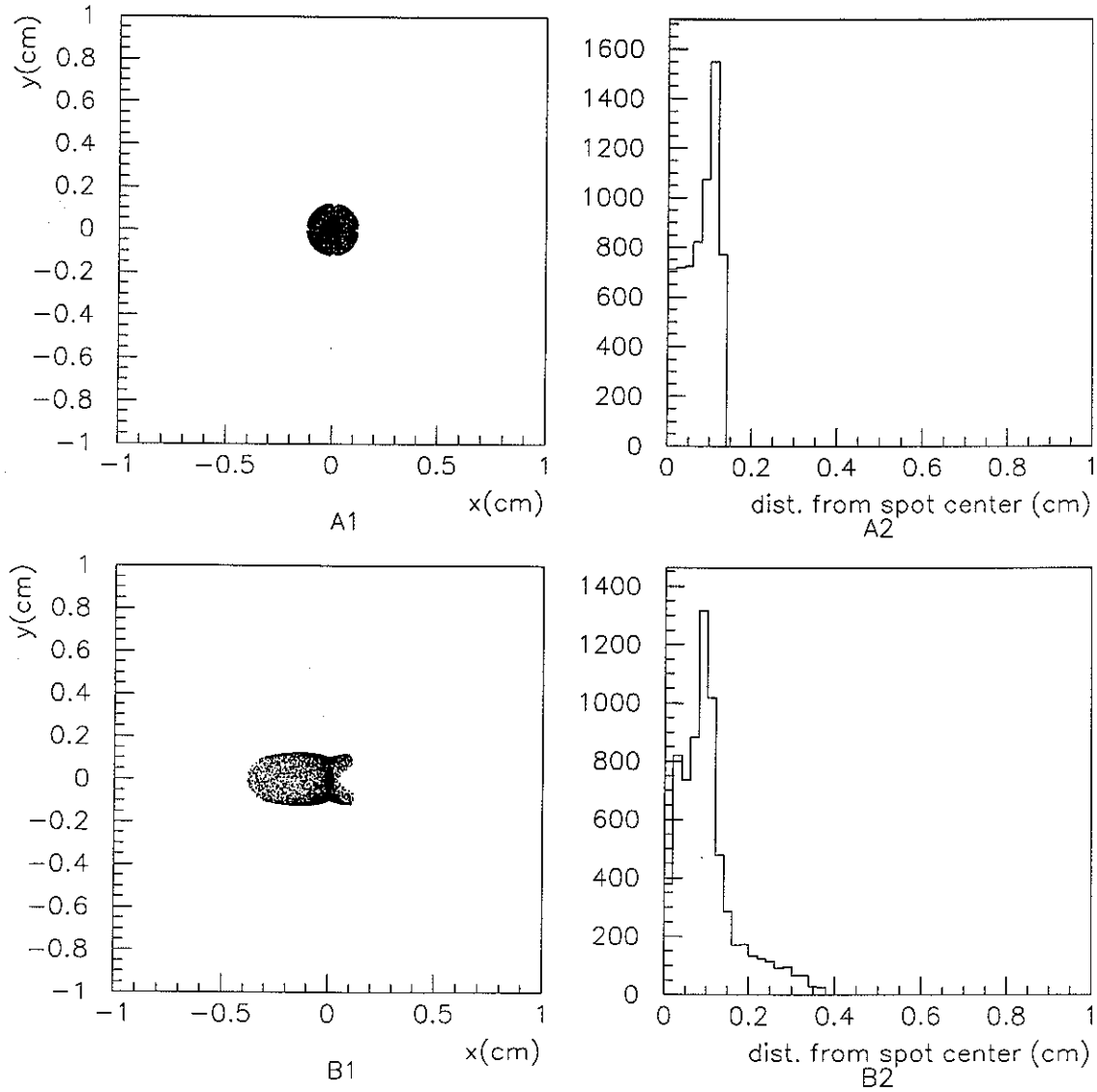

Figure 4: Projection of figure of the spot on the spherical PMT's cluster at the focal plane for a Schmidt camera with corrector plate type II, with incidence angles of 0^o (fig. A1) and 20^o (fig. B1). Figures A2 and B2 are the corresponding radial distribution of the spot size.

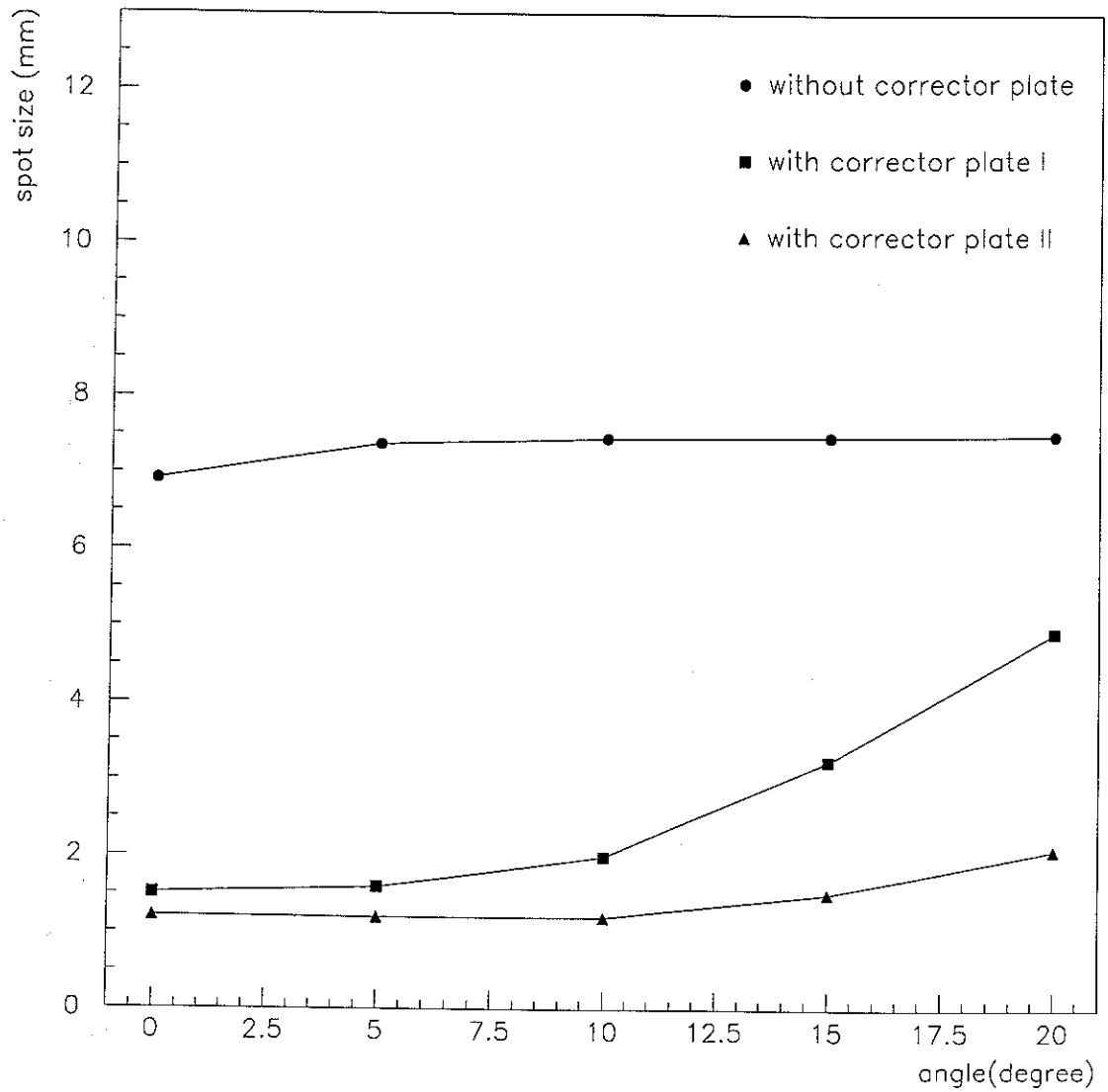

Figure 5: Spot size as a function of the incidence angle for the Schmidt system with and without corrector plate.

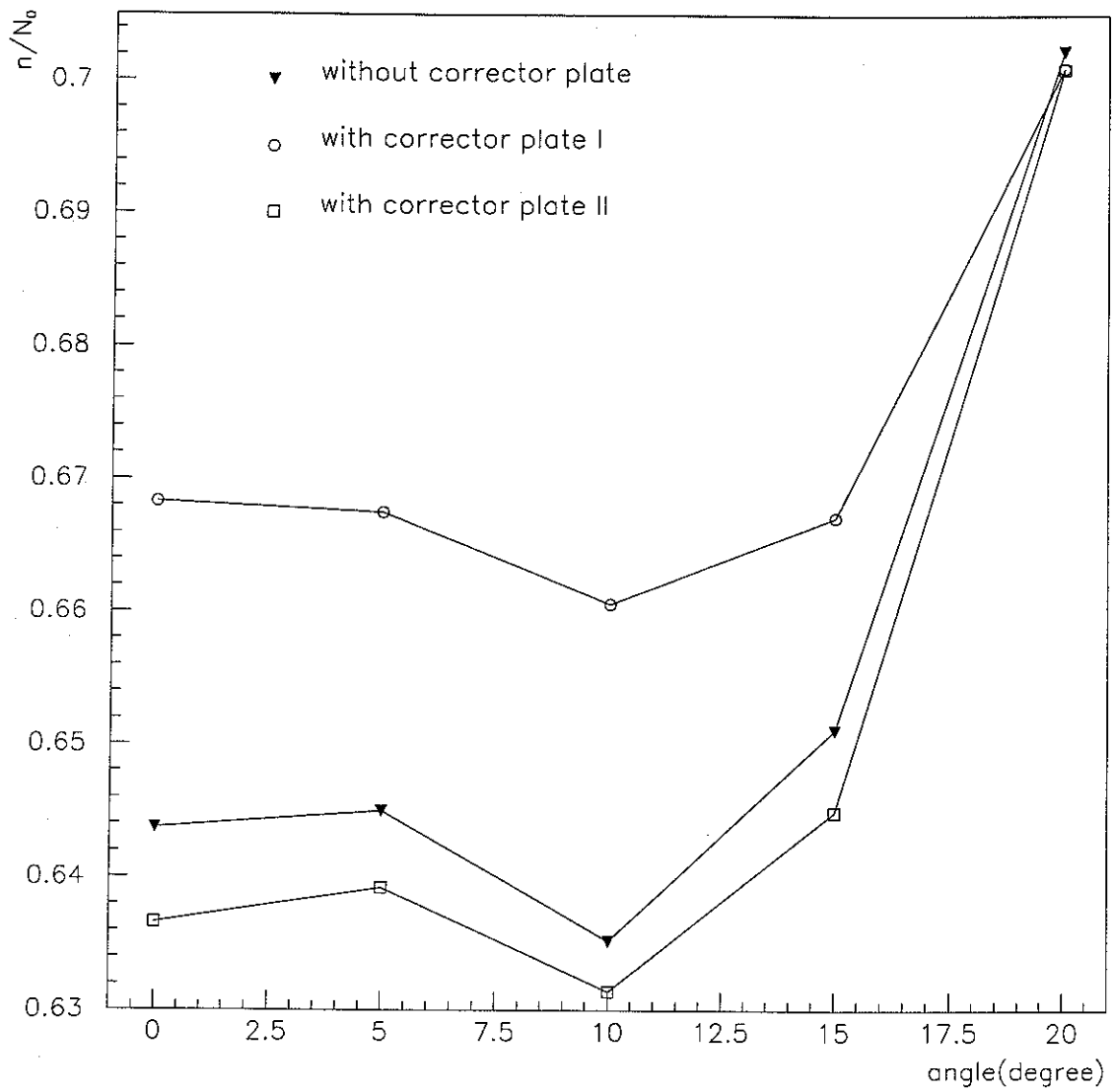

Figure 6: Ratio between the number of rays that reached the cluster of PMT's and the number of rays that reached the optical system.

4 Area Obscured by the PMT's Cluster

Imagine a plane which is perpendicular to the propagation direction of the light and cross by the center of the diaphragm. When a ray of light reaches this plane at a point with distance r to the center of the diaphragm, this ray will arrive (after being reflected by the mirror) at the position $d(r)$ above some given surface S, related with the ray of light that cross by the center of the diaphragm with the same direction. If that surface were the focal surface of the optic system, $d(r)$ will be the function showed in figure 7.A.

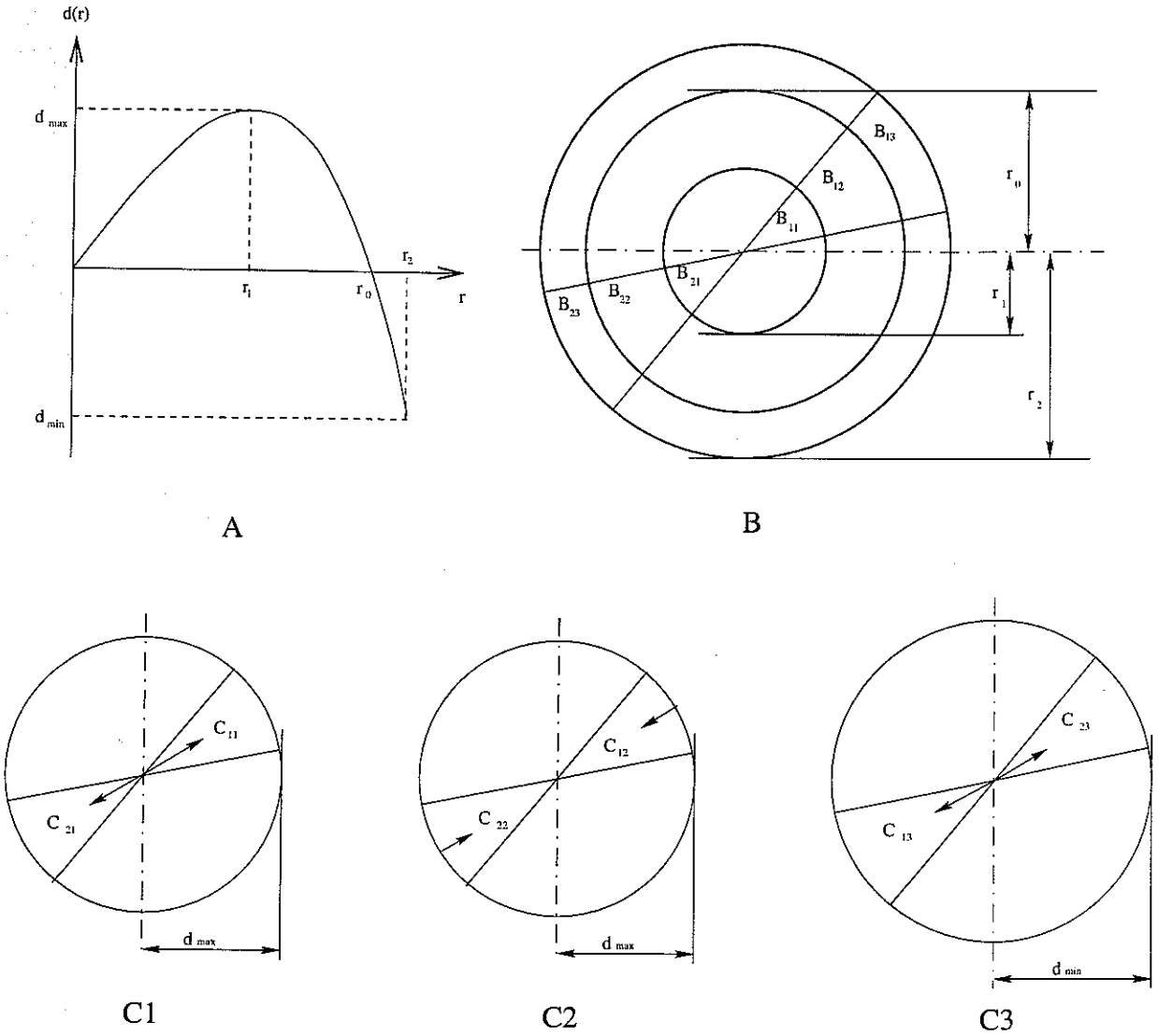

Figure 7: Schematic representation of figure formed at focal surface (C1, C2, C3) by the incident rays at the diaphragm's region (B), as in the graphic of $d(r)$ (A).

The plane we talk about in the last paragraph was divided in sectors (fig.7B), and

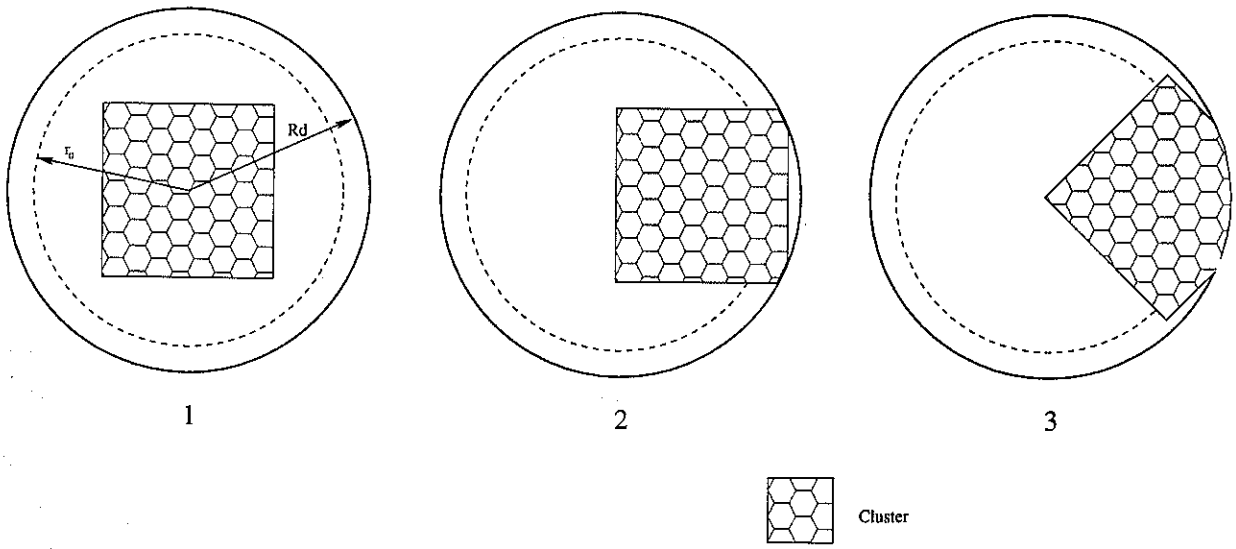

Figure 8: Schematic representation of the shadow caused by the cluster of PMT's.

(figs.7C) shows what happens with the figure at the focal surface, the arrows shows if the figure increase or decrease when r increase.

In concordance with fig. 1, the region obscured by the cluster for small angles of incidence is showed in fig. 8.1 which encloses principally $r < r_1$, and consequently not great effects are observed in the figure above the cluster, besides four small "weaker" regions that are provoked by the regions closer to the cluster vertex.

In the case of great e incidence angles, the effects of the cluster are notorious, as we see in figs. 2.B1–4.B1. This is caused by two effects as follow. First, it is due to the cluster of PMT's can obscure a integer sector and produce a clear effect in figure formed in focal surface (see figure 8.2 and 8.3). Second is because the opposite sector to the obscured area, with $r > r_0$, that give a small contribution, caused by signal inversion of $d(r)$ as showed in figure 7.B (sector B_{13} and B_{23}) and 7.C. Furthermore, due to large angle, the circular shape of diaphragm form a elliptical figure in the plate cited above, this gives a figure in focal surface that is approximately circular elliptical, not as showed in figure7.C.

For the case of Schmidt camera with corrector plate, these effects are similar, but we should consider the fact that the corrector plate deforms a little the figure at the focal surface.

5 Results

We can see from figures 2–4, that the spot size radius obtained are a little smaller than the ones obtained in ref. [3]. For example, considering an incidence angle of 20^o, where the difference is more notorious, we have $R_{spot} \simeq 6.92mm$ for the Schmidt camera without corrector plate. In ref. [3], the value of the spot size in the same situation is $9.3mm$. This

behavior is similar when the Schmidt camera have the corrector plate type I or II (In this work: $R^I_{spot} \simeq 4.92mm$ and $R^{II}_{spot} \simeq 2.08mm$, and in ref. [3]: $R^I_{spot} \simeq 8.2mm$ and $R^{II}_{spot} \simeq 4.5mm$). This spot size decreasing should be due to the difference in the definition of spot size (we defined R_{spot} as the radio that encloses 90% of the rays whereas in ref. [3] encloses the 100% of the rays), and of some parameters between the two simulated cameras. With the objective of simulating the final design of the Schmidt camera, we considered $R_{mirror} = 3.4m$ and $R_{dia} = 0.85m$, while in ref. [3], the value of these parameters are $R_{mirror} = 3.0m$ and $R_{dia} = 0.83m$. This means that there is a strong dependence of the spot size with the R_{mirror}/R_{dia} ratio. However, the dependence of the spot size with incident angle (with and without corrector plate) is very similar to the results of Matthias and Privitera's work. Furthermore, we also simulated the Schmidt camera with the same parameters of ref. [3] and we obtained good concordance.

Another effect well defined that we can see is the presence of a region obscured (shadow) by the PMT's cluster, principally for greater incidence angles (figs. 2–4). Does this shadow will be relevant for the reconstruction of the EAS? In the case of the Schmidt camera without corrector plate with incidence angles of 20^o, the propagation of about $6mm$ corresponds to 1/10 of the pixel surface approximately, and this could change, in a significant way, the time structure of the passage of the signal seen by the pixel.

Figure 6 shows that the Schmidt camera with corrector plate type I has an effective area a little bigger than the other cases (Schmidt camera without corrector plate and with corrector plate type II). This effect could be explained by the decreasing of the curvature radius of the focal surface when using corrector plate type I, this provokes a small reduction of the region obscured by the PMT's cluster.

6 Conclusions

In this work we developed a ray-tracing program in order to simulate the optic of the Auger project fluorescence detector. We showed that the introduction of corrector plates reduces the spot size at the focal surface and it has the same qualitative behavior with the incidence angle obtained by Matthias and Privitera [3]. It is important to note that we have simulated the optical system with the final parameters of the fluorescence detector ($R_{mirror} = 3.4m$ and $R_{dia} = 0,85m$). In addition, we have simulated the Schmidt camera with the parameters of ref. [3] and we obtained a good concordance.

Furthermore, we observed the presence of a shadow provoked by the PMT's cluster. This shadow may be relevant to the crossing time of the signal seen by the photocathode.

Acknowledgments

We would like to thanks to prof. Carlos Escobar for his ideas and suggestions. One of us (H.C.R.) is grateful for the hospitality of Nuclear Physics Department, University of São Paulo, where part of this work was done. This work was supported by Fundação

de Amparo à Pesquisa do Estado de São Paulo (FAPESP) and Conselho Nacional de Desenvolvimento Científico e Tecnológico (CNPq), Brazil.

References

[1] *The Pierre Auger Observatory - Design Report* (March 1997).

[2] M. Born and E. Wolf, *Principles of Optics*, Sec. 6.4.

[3] G. Matthiae and P. Privitera, *Auger Tecnical Note*, GAP-98-039.